



UNIVERSITY OF LEEDS

This is a repository copy of *Observed dynamic soil–structure interaction in scale testing of offshore wind turbine foundations*.

White Rose Research Online URL for this paper:  
<http://eprints.whiterose.ac.uk/80835/>

---

**Article:**

Bhattacharya, S, Nikitas, N, Garnsey, J et al. (5 more authors) (2013) Observed dynamic soil–structure interaction in scale testing of offshore wind turbine foundations. *Soil Dynamics and Earthquake Engineering*, 54. 47 - 60. ISSN 0267-7261

<https://doi.org/10.1016/j.soildyn.2013.07.012>

---

**Reuse**

Unless indicated otherwise, fulltext items are protected by copyright with all rights reserved. The copyright exception in section 29 of the Copyright, Designs and Patents Act 1988 allows the making of a single copy solely for the purpose of non-commercial research or private study within the limits of fair dealing. The publisher or other rights-holder may allow further reproduction and re-use of this version - refer to the White Rose Research Online record for this item. Where records identify the publisher as the copyright holder, users can verify any specific terms of use on the publisher's website.

**Takedown**

If you consider content in White Rose Research Online to be in breach of UK law, please notify us by emailing [eprints@whiterose.ac.uk](mailto:eprints@whiterose.ac.uk) including the URL of the record and the reason for the withdrawal request.



[eprints@whiterose.ac.uk](mailto:eprints@whiterose.ac.uk)  
<https://eprints.whiterose.ac.uk/>

## **Observed Dynamic Soil-Structure Interaction in scale testing of Offshore Wind Turbine Foundations**

S.Bhattacharya<sup>1</sup>, N.Nikitas<sup>2</sup>, J.Garnsey<sup>3</sup>, N.A. Alexander<sup>4</sup>, J.Cox<sup>5</sup>, D. Muir Wood<sup>6</sup> and D. F.T.Nash<sup>7</sup>

<sup>1</sup> Chair of Geomechanics, University of Surrey

<sup>2</sup> Lecturer, University of Leeds

<sup>3</sup> Head of Civil Engineering, RWE Innogy

<sup>4</sup> Senior Lecturer, University of Bristol

<sup>5</sup> Research student, University of Bristol

<sup>6</sup> Professor of Geotechnical Engineering, University of Dundee

<sup>7</sup> Senior lecturer, University of Bristol

Number of words: 4885 (main text)

Number of tables: 5

Number of figures: 14

*Correspondence author:*

Professor Subhamoy Bhattacharya

University of Surrey

United Kingdom

Email: [S.Bhattacharya@surrey.ac.uk](mailto:S.Bhattacharya@surrey.ac.uk)

**Abstract:**

Monopile foundations have been commonly used to support offshore wind turbine generators (WTGs), but this type of foundation encounters economic and technical limitations for larger WTGs in water depths exceeding 30m. Offshore wind farm projects are increasingly turning to alternative multipod foundations (for example tetrapod, jacket and tripods) supported on shallow foundations to reduce the environmental effects of piling noise. However the characteristics of these foundations under dynamic loading or long term cyclic wind turbine loading are not fully understood. This paper summarises the results from a series of small scaled tests (1:100, 1:150 and 1:200) of a complete NREL (National Renewable Energy Laboratory) wind turbine model on three types of foundations: monopiles, symmetric tetrapod and asymmetric tripod. The test bed used consists of either kaolin clay or sand and up to 1.4 million loading cycles were applied. The results showed that the multipod foundations (symmetric or asymmetric) exhibit two closely spaced natural frequencies corresponding to the rocking modes of vibration in two principle axes. Furthermore, the corresponding two spectral peaks change with repeated cycles of loading and they converge for symmetric tetrapods but not for asymmetric tripods. From the fatigue design point of view, the two spectral peaks for multipod foundations broaden the range of frequencies that can be excited by the broadband nature of the environmental loading (wind and wave) thereby impacting the extent of motions. Thus the system lifespan (number of cycles to failure) may effectively increase for symmetric foundations as the two peaks will tend to converge. However, for asymmetric foundations the system life may continue to be affected adversely as the two peaks will not converge. In this sense, designers should prefer symmetric foundations to asymmetric foundations.

**Keywords:** Dynamics, Soil-structure Interaction, Offshore Wind Turbines, Frequency

**Nomenclature:**

E	Young's Modulus of caisson skirt
t	Thickness of caisson skirt
h	Caisson depth
G	Shear modulus of surrounding soil
D	Diameter of the caisson or pile
$H_{max}$	Bearing capacity in horizontal direction
$V_{max}$	Bearing capacity in vertical direction
V	Vertical load
H	Horizontal load
$\gamma'$	Buoyant soil unit weight
$f_b$	Natural frequency of the blades (Hz)
$f_f$	Forcing frequency (Hz)
$f_n$	Natural frequency (Hz)

L	length of tower
$\sigma_{\theta}$	Hoop stresses
p	Soil pressure
$s_u$	Undrained shear strength
$k_h$	Horizontal coefficient of soil permeability
P	Horizontal load
y	Distance between foundation and load application
$\sigma_y$	Pile yield stress
$t_w$	Pile wall thickness
$M_1$	Mass of foundation frame
$M_2$	Mass of tower
$M_3$	Mass of onboard machinery
m	Mass of one blade
$M_{sum}$	Cumulative mass of the foundation, tower, onboard machinery and a blade
M	Mass per unit length
$a_n$	Modal number parameter

## 1.0 INTRODUCTION:

The design and construction of foundations for offshore turbines are challenging because of the harsh environmental conditions and as a result provide a focus of major research in Europe, see for example Achmus et al (2009), Kuo et al (2012), Cuellar et al (2012). The UK has also embarked on a massive scheme of investment in offshore wind power development to meet future energy challenges. Currently, 1.5GW of electricity comes from offshore wind farms, but to meet the EU target an additional 28GW will be required by 2020. This would lead to the construction of over 6000 separate turbine structures in the next 10 years, requiring a massive increase in installation capacity. The scale of this challenge is illustrated in

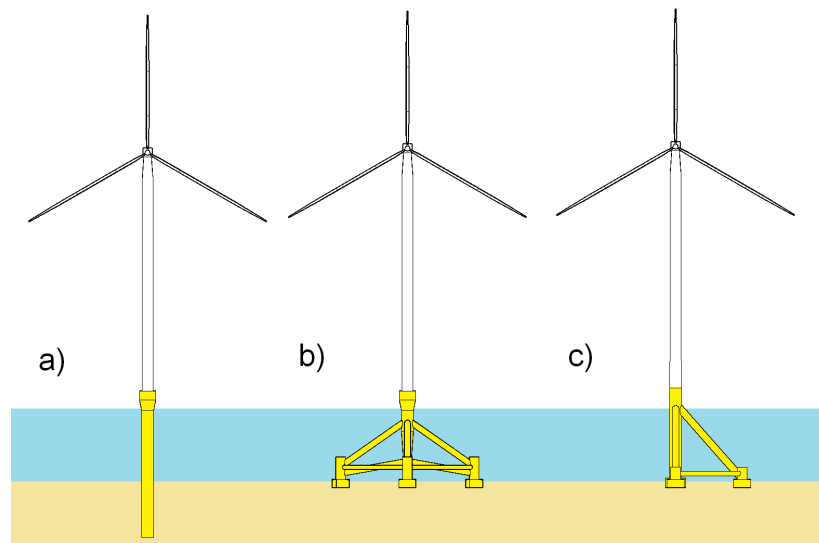


Figure 1: A schematic diagram showing different types of foundations: (a) monopile; (b) tetrapod; (c) Asymmetric tripod

Table 1: Current and future offshore wind farm statistics (EWEA,2012)

	End 2011	By 2020
Total power production capacity	2 GW	29GW
Number of wind turbines	636	6000+
Rate of turbine installation required	1 every 11 days	2.5 per day
Depth of water	~ 10-20m	30 – 60m (round 3)
Distance from shore	< 30 km	Up to 205 km

Furthermore, the wind farms that will be created as part of this offshore development will be situated in far deeper water than existing wind farms. The majority of operational offshore wind-turbines situated in UK waters (Rounds 1 and 2) are founded on monopiles in water depths up to 35 meters. However, these foundations may not be competitive for larger wind turbine generators in water

depths over 30m due to the increased costs and risks associated with their fabrication, transportation and installation processes.

Therefore, other types of foundations such as three and four leg jackets, tripods, tripiles and tetrapods are increasingly being designed and deployed. Furthermore environmental drivers are leading to increasing research and development of suction caisson foundations beneath these structures which avoid the noise impact associated with piling. Whilst such foundation/substructure combinations have previously been used in the oil and gas industry typically to support Minimum Facilities Platforms, riser towers, suction anchors and the like, there is relatively little experience of the dynamic soil-structure interaction of these foundations under loading from wind turbine generators. Figure 1 shows the schematic diagram of a range of foundations either in use or proposed for offshore wind turbines.

To date there has been no long-term observations of the performance of these relatively novel structures. On the other hand, monitoring of a limited number of offshore wind turbines supported on monopiles has indicated a departure of the system dynamics from their design assumptions (Kuhn, 2000). This paper summarises the results from a series of small scaled tests of a typical wind turbine supported on three types of foundations: monopiles (1a), tetra-pod suction caisson foundation (1b), asymmetric tripod suction caisson foundation (1c). The focus of the study is on dynamic characterisation of these structures (dynamic characterisation being interpreted as the free vibration response of the system and its relation to the forcing frequencies applied to the system). The study highlights the difference in dynamic behaviour between monopile and multipod type of foundations. It will be shown that the different dynamic behaviour is crucial for long term performance of these structures.

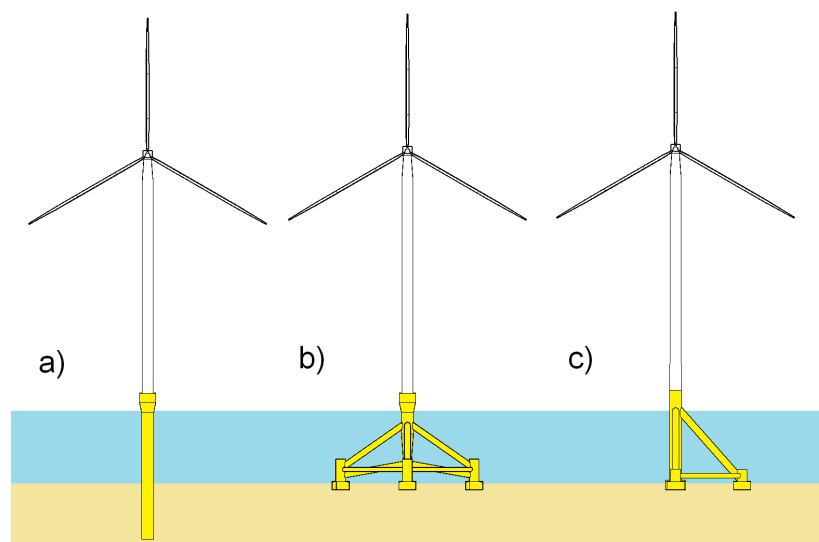


*Figure 1: A schematic diagram showing different types of foundations: (a) monopile; (b) tetrapod; (c) Asymmetric tripod*

## 2.0 DYNAMIC CONSIDERATIONS IN DESIGN OF WIND TURBINE FOUNDATIONS

As a result of their slender nature, offshore wind-turbines are dynamically sensitive at low frequencies, the first modal frequency of the system (less than 1Hz) being very close to the excitation frequencies imposed by environmental and mechanical loads. Figure 2 shows the main frequencies for a three-bladed National Renewable Energy Laboratory (NREL) standard 5MW wind turbine with an operational interval of 6.9 to 12.1 rpm. The rotor frequency (often termed 1P) lies in the range 0.115-0.2Hz and the corresponding 'blade passing frequency' for a three-bladed turbine lies in the range 0.345-0.6Hz. The figure also shows typical frequency distributions for wind and wave loading. The peak frequency of typical North Sea offshore waves is about 0.1Hz.

It is clear from the frequency content of the applied loads that the designer of the turbine and foundation has to select a system frequency (the global frequency of the overall wind turbine-foundation system) which lies outside this range of frequencies in order to avoid system resonance. The usual choice for fixed wind turbines would lie in the interval between turbine and blade passing frequencies (referred to as a 'soft-stiff' structure). Other definitions of "soft-soft" and "stiff-stiff" can be found in Bhattacharya et al (2012).

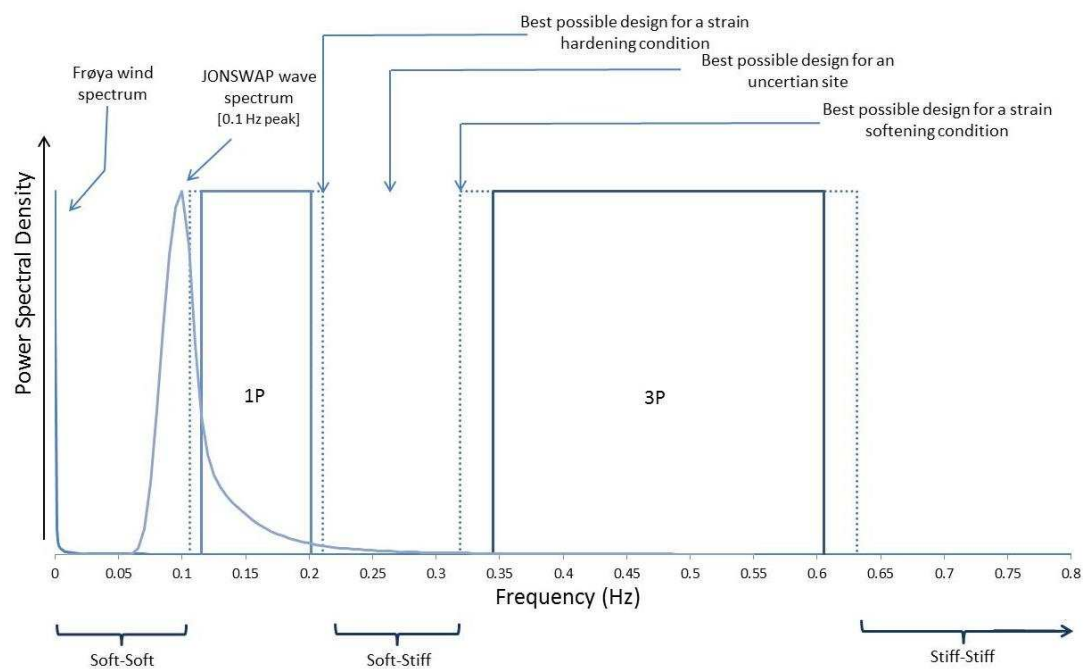


Figure 2: Forcing frequencies plotted against the power spectral densities for a 3 bladed NREL standard 5W Wind turbine. 3P stands for blade passing frequency

It is considered useful to review the relevant codes of practice. DNV Guidelines (2002) suggest that the natural frequency of the wind turbine should not come close to the likely forcing frequencies arising from imposed environmental loads. It is also specified that the global frequency of the system should be at least  $\pm 10\%$  away from

operational 1P and 2P/3P frequencies, as indicated by the dotted lines in Figure 2. 2P and 3P relate to blade passing frequencies for 2 bladed and 3 bladed wind turbines.

Small scale 1-g tests reported by Lombardi (2010), Bhattacharya et al (2012), Bhattacharya et al (2011), Cox et al (2011) showed that the natural frequency of a wind turbine system changes with cycles of loading. The main reason for this change is the alteration of the foundation stiffness due to strain-hardening or strain-softening behaviour of the soil supporting the foundation owing to the loading cycles.

The main conclusions drawn from the study can be summarised as follows:

- a) For strain-hardening sites (for example, loose to medium dense sand) where the stiffness of the soil increases with cycles of loading, the natural frequency of the overall system will increase.
- b) For strain-softening sites (clay sites) where the stiffness of the soil may decrease with cycles of loading, the natural frequency of the overall system will also decrease correspondingly. Of course, this depends on the strain level in the soil next to the pile and the number of cycles.

These conclusions have been supported by evidence of limited field measurements at Lely Island reported by Kuhn (2000). Cyclic element tests on soil showing stiffness increase, and cyclic tests on foundations alone have also corroborated these conclusions.

#### ***How much frequency change can be allowed?***

From a number of site surveys of offshore wind farms it was observed that the sub-sea sediment at an offshore site can vary significantly. In many cases it is composed of a number of discrete layers with differing properties. It is envisaged that high quality element tests can provide us with guidance on the nature of the site, i.e. whether it will be strain-hardening or strain-softening under cyclic loading. Three cases may arise:

- (a) The site is known to be strain-hardening. Theoretically, the best design for such a site is to place the natural frequency of the system 10% higher than the highest 1P frequency), leading to the maximum allowable frequency change interval spanning up to the next resonance limit at the 2P/3P frequency.
- (b) The site is known to be strain-softening. The designer may aim to place the natural frequency at 10% lower than the lowest 2P/3P frequency value.
- (c) This is an unknown site and the behaviour cannot be predicted. The design is best optimised if the natural frequency is in the centre between 1P and 2P/3P frequencies.

Table 2 shows the details of a few types of turbines and the corresponding estimated percentage of allowable frequency change according to above. It is therefore clear that a certain amount of change in natural frequency is acceptable without seriously compromising the performance.

*Table 2: Details of the various turbines manufacturers*

Turbine make and details	Rating (MW)	Cut in (Hz)	Cut out (Hz)	% natural frequency change allowed for a strain-hardening site	% natural frequency change allowed for a strain-softening site	% natural frequency change allowed for an unknown site
RE Power 5M	5.075	0.115	0.201	40%	28%	17%
RE Power 6M	6.15	0.128	0.201	56%	36%	22%
Vestas V90	3	0.143	0.306	15%	13%	7%
Vestas V120	4.5	0.165	0.248	63%	39%	24%
NREL 5 MW	5	0.115	0.201	40%	28%	17%

In this respect there are three design challenges:

- (a) The foundation stiffness must be estimated very accurately from the available soil data for estimation of natural frequency of the system. This is significantly more challenging than the ULS (Ultimate Limit State of Collapse) design, where conservatism is safe i.e. the soil parameters can be under estimated.
- (b) The potential for change in foundation stiffness with time as a result of cyclic loading must be understood so that the risk of the system frequency coinciding with a loading frequency can be minimised.
- (c) While a given change in natural frequency may be acceptable over the life time of the structure, it is necessary to understand if that change is gradual or sudden. This will have a major influence in accurately estimating the ensuing response amplitudes and subsequently the structure's life expectancy.

The next section of the paper will explore the answers to some of these questions through scaled model testing at BLADE [Bristol Laboratories for Advanced Dynamics Engineering].

### **3.0 EXPERIMENTAL MODELLING:**

The main purposes of the experimental testing are as follows:

1. To characterise the free dynamics of the system: the free vibration characteristics of the wind turbine system including the foundation flexibility i.e. natural frequency and damping.
2. To study the effect of cyclic loading on the natural frequency of the system through uniform loading (sine waves) and random loading (white noise).
3. To understand whether or not the total wind turbine system (including the flexibility of the foundation) is non-linear having varying stiffness with the response amplitude.

Modelling the dynamics of offshore wind turbines is very complex and involves various interactions. The main interactions are summarised below.

1. Vibration of the tower resulting from interactions with the dynamic loads (wind, wave, 1P, 3P and the corresponding randomness of the loads)
2. Vibrations of the blade and their transfer to the tower
3. Foundation-soil interaction resulting from the cyclic/dynamic loading on the foundation

Derivation of scaling laws for 1-g modelling of monopile supported wind turbines can be found in Bhattacharya et al (2011), Lombardi et al (2013). In the study the six non-dimensional groups were derived based on the following physical mechanisms:

- 1) The strain field in the soil around a laterally loaded pile which will control the variation of soil stiffness
- 2) The cyclic stress ratio in the soil in the shear zone
- 3) The rate of soil loading which will influence the dissipation of pore water pressure
- 4) The system dynamics, the relative spacing of the system frequency and the loading frequency
- 5) Bending strain in the monopile foundation for considering the non-linearity in the material of the pile
- 6) Fatigue in the monopile foundation

The above non-dimensional groups originally developed for monopiles by Bhattacharya et al (2011) were also used to analyse symmetric tetrapod foundations (Bhattacharya et al 2012). However later, while studying asymmetric tripod foundations, it was realised that additional scaling relations are necessary to take into account the geometric arrangement (i.e. characterising the asymmetry). Thus, this section of the paper incorporates the additional scaling laws required to study generic multipod foundations.

The rules of similarity between the model and prototype that need to be maintained are:

1. *Geometric similarity*: The dimensions of the small scale model need to be chosen in such a way that similar modes of vibration will be excited in model and prototype. It is expected that rocking modes will govern the multi-pod (tripod or tetrapod suction piles or caissons) foundation and as a result relative spacing of individual pod foundations ( $b$  in Figure 3) with respect to the tower height ( $L$  in Figure 3) needs to be maintained, see equation 1. This geometrical scaling is also necessary to determine the point of application of the resultant force on the model. The aspect ratio of the caisson (diameter to depth ratio) should also be maintained to ensure the pore water flow is reproduced, details can be found in Bhattacharya et al (2011). This leads to the similitude relationship given by equation 2.

$$\left(\frac{L}{b}\right)_{\text{model}} = \left(\frac{L}{b}\right)_{\text{prototype}} \quad (1)$$

where L is the length of the tower and b is the spacing of the caissons

$$\left(\frac{D}{h}\right)_{\text{model}} = \left(\frac{D}{h}\right)_{\text{prototype}} \quad (2)$$

where D is the diameter of the caisson and h is the depth of the caisson.

2. *Mass distribution similarity*: In order to model the vibration of the tower, the mass distribution between the different components needs to be preserved. In other words the ratios  $M_1 : M_2 : M_3 : m$  in Figure 3 need to be maintained in model and prototype.

$$(M_1 : M_2 : M_3 : m)_{\text{model}} = (M_1 : M_2 : M_3 : m)_{\text{prototype}} \quad (3)$$

3. *Relative stiffness between suction caisson and the surrounding soil*: The stiffness of the caissons relative to the soil needs to be preserved in the model so that the caisson interacts similarly with the soil as in the prototype. Caisson flexibility affects both the dynamics and the soil structure interaction and as a result this mechanism is of particular interest. Based on the work of Doherty et al (2005) the non-dimensional flexibility of a suction caisson is given by:

$$\frac{Et}{GD} \quad (4)$$

where

E = Elastic modulus of caisson skirt (GPa)

t = Thickness of caisson skirt (mm)

G = Shear modulus of surrounding soil (GPa)

D = Diameter of the caisson (m)

The above group can be derived from the expression of hoop stress ( $\sigma_\theta$ ) developed in a thin walled cylindrical pressure vessel given by equation 5.

$$\sigma_\theta \propto \frac{pD}{t} \quad (5)$$

noting that  $\sigma_\theta$  is the stress in the caisson which is proportional to the elastic modulus of caisson skirt (E) and p is the pressure applied by the soil, dependent on the shear modulus (G). Therefore the following relationship should be maintained:

$$\left(\frac{Et}{GD}\right)_{\text{model}} = \left(\frac{Et}{GD}\right)_{\text{prototype}} \quad (6)$$

4. *Vertical load and lateral load combination*: The loading encountered in a single caisson in a multipod foundation (Figure 1b and 1c) is a combination of

vertical and horizontal load. For a combination of lateral and vertical load, a failure envelope given by equation 7 is often used in practice.

$$\left(\frac{V}{V_{\max}}\right)^i + \left(\frac{H}{H_{\max}}\right)^j = 1 \quad (7)$$

where

$H_{\max}$  = Bearing capacity in horizontal direction

$V_{\max}$  = Bearing capacity in vertical direction

$V$  = Vertical load on the individual caisson

$H$  = Horizontal load on the caisson

and Senders and Kay (2002) suggest  $i = j = 3$ .

The non-dimensional group to preserve is  $\frac{V}{V_{\max}}$  which is proportional to

$\frac{V}{\gamma' D^3}$  for sandy soil where  $\gamma'$  is the buoyant soil unit weight (KN/m<sup>3</sup>) and  $D$

is the caisson diameter (m). The relationship for clay soil is given by equation 8c. Therefore the following relationship should hold:

$$\left(\frac{V}{V_{\max}}\right)_{\text{model}} = \left(\frac{V}{V_{\max}}\right)_{\text{prototype}} \quad (8a)$$

$$\left(\frac{V}{\gamma' D^3}\right)_{\text{model}} = \left(\frac{V}{\gamma' D^3}\right)_{\text{prototype}} \quad \text{for sandy soil} \quad (8b)$$

$$\left(\frac{V}{s_u D^2}\right)_{\text{model}} = \left(\frac{V}{s_u D^2}\right)_{\text{prototype}} \quad \text{for clay soil} \quad (8c)$$

The lateral load acting on the caisson can be derived from the cyclic stress ratio in the shear zone next to the footing which is quite similar to the case for pile as derived in Bhattacharya et al (2011). This leads us to a non-dimensional group (equation 9) that must be satisfied. This group will dictate the rate of cyclic accumulation of strain.

$$\left(\frac{H}{GD^2}\right)_{\text{model}} = \left(\frac{H}{GD^2}\right)_{\text{prototype}} \quad (9)$$

5. *Damping of the system:* The damping of a structure also has a significant effect on the motions experienced by the structure under dynamic loading conditions. As a result the regime of damping of the prototype system should be replicated by that of the model system: critical damping, under-damping or over-damping. This has been ensured by maintaining constant the damping ratio of both systems.

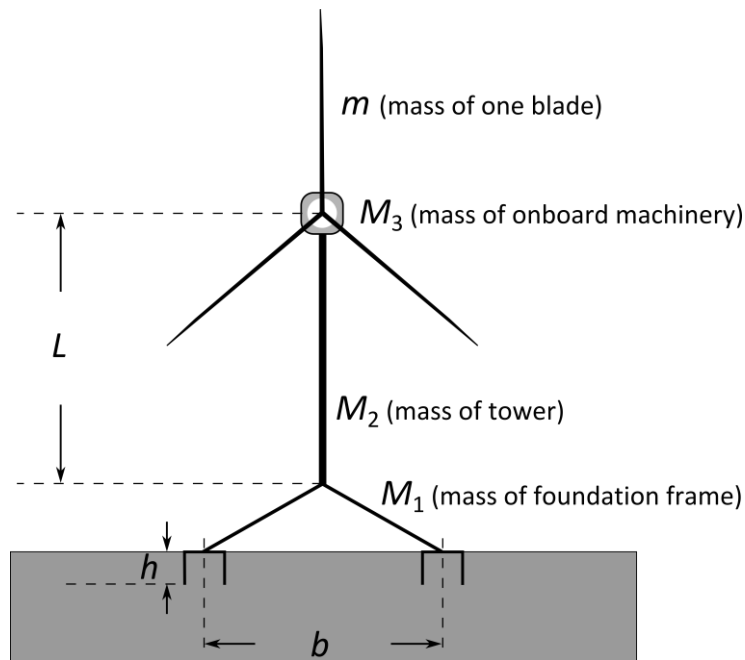


Figure 3: Schematic diagram for multi-pod foundation wind turbines

The non-dimensional groups derived are summarised in Table 3. Table 4 lists typical values of these groups for a limited number of suction caissons whose properties are available in the public domain. The spacing of suction caissons, masses of tripod frame and jacket are taken based on design values.

Table 3: Scaling laws for studying the dynamics of wind turbines considering Soil Structure Interaction

Name of the non-dimensional group	Physical meaning	Remarks
$\left(\frac{L}{b}\right)$	This is to excite similar modes of vibration and apply proportional moment loading to the model	Geometric scaling of length. This is applicable for caisson foundations.
$\left(\frac{D}{h}\right)$	Aspect ratio of a caisson to have similar flow and proportional soil resistance (shaft and end-bearing)	Geometric similarity of the model. This is mostly applicable to caisson foundations
$(M_1 : M_2 : M_3 : m)$	Proportional mass distribution along the length of the model	Mass distribution similarity
$\left(\frac{Et}{GD}\right)$	Flexibility of the caisson skirts so as to have similar soil-structure interaction	This is applicable to caisson foundations
$\left(\frac{H}{GD^2}\right)$	Strain field in the soil around the pile and Cyclic Stress Ratio (CSR) in the shear zone i.e. ratio of shear stress to the vertical effective stress at a particular depth	Similar strain field which will control the degradation of soil stiffness

Name of the non-dimensional group	Physical meaning	Remarks
$\left(\frac{V}{V_{\max}}\right)$	Having similar factor of safety on vertical bearing capacity	This is applicable to caisson foundations or shallow foundations
$\left(\frac{k_h}{f_f D}\right)$	Rate of loading	Modelling consolidation and the dissipation of pore water pressure. Details discussion can be found in Bhattacharya et al (2011)
$\left(\frac{f_f}{f_n}\right)$	Relative spacing of the forcing frequencies and the natural frequencies	System dynamics. This group takes care of the overall stiffness of the system. Details discussion can be found in Bhattacharya et al (2011)
$\left(\frac{f_b}{f_n}\right)$	Relative spacing of the blade natural frequency and the overall natural frequency	Interaction between the tower modes and blade modes
$\left(\frac{P_y}{ED^2 t_w}\right)$	Bending strain in the pile	Non-linearity in the material of the pile. Details discussion can be found in Bhattacharya et al (2011).
$\left(\frac{P_y}{\sigma_y D^2 t_w}\right)$	Stress level in the pile	Fatigue limit state. Details discussion can be found in Bhattacharya et al (2011).

Table 4: Values of typical prototype turbine values

Non-dimensional group	Prototype	Remarks
$\left(\frac{L}{b}\right)$	2 to 3	L = Height of tower = 90m b = Spacing of caissons for a asymmetric tripod = 45m (typical) b = Spacing of caissons for a typical jacket = 30m
$\left(\frac{D}{h}\right)$	1 to 2	<u>Frederikshavn offshore wind farm site:</u> D = Diameter of the caisson = 12m h = depth of the caisson = 6m <u>Wilhelmshaven offshore wind farm site:</u> D = Diameter of the caisson = 16m h = depth of the caisson = 15m
$(M_1 : M_2 : M_3 : m)$ $M_{\text{sum}} = M_1 + M_2 + M_3 + m$	$M_1 = 63\% M_{\text{sum}}$ $M_2 = 18\% M_{\text{sum}}$	<u>For a tripod,</u> $M_1$ (Mass of the foundation frame) = 1200 tonnes $M_2$ (Mass of the tower ) = 350tonnes (NREL) $M_3$ (Mass of the nacelle including rotor) =

	$M_3 = 16\% M_{sum}$  $m = 3\% M_{sum}$	300tonnes (NREL) $m$ (Mass of one blade) = 18tonnes (typical) For a typical jacket: $M_1$ (Mass of the jacket) = 1000 tonnes
$\left(\frac{Et}{GD}\right)$	8.5 to 15	For the Frederikshavn offshore wind farm site the value is around 15 For Wilhelmshaven offshore wind farm site, the value is around 8.5
$\left(\frac{V}{\gamma D^3}\right)$	0.18 to 0.24	For Frederikshavn site the value is around 0.24 For Wilhelmshaven site, the value is around 0.18

**Designing experiments:**

Using the scaling laws detailed above the experiments can subsequently be designed. Once the total vertical load is known given by equation 8a, the mass distribution given by equation 3 needs to be maintained. Three asymmetric tripods (1:200, 1:150 and 1:100) and one tetrapod (1:100) were designed, built and tested. The mass distributions of the models are given in Table 5. It must be mentioned that the three scaled models do not represent the same prototype as the soil test beds were different. As the main aim of the paper is to characterise the dynamics of the system, only the relevant groups are described in this section.

Table 5: Mass distribution of the differently scaled models (see Table 4).

Type of foundation	Mass of the components
Asymmetric Tripod	1:100 scale [ $M_1 = 1.90\text{kg}$ , $M_2 = 0.55\text{kg}$ , $M_3 = 0.5\text{kg}$ , $m = 0.08\text{kg}$ ]
	1:150 scale [ $M_1 = 4.58\text{kg}$ , $M_2 = 1.89\text{kg}$ , $M_3 = 2.59\text{kg}$ , $m = 0.34\text{kg}$ ]
	1:200 scale [ $M_1 = 2.60\text{kg}$ , $M_2 = 1.1\text{kg}$ , $M_3 = 1.5\text{kg}$ , $m = 0.2\text{kg}$ ]

**Experimental setup:**

This section will describe the different types of setup used in this study. Figure 4 shows the setup for 3 types of wind turbine systems. All the tests were carried out at BLADE [Bristol Laboratory for Advanced Dynamics Engineering] in a soil container having rigid boundaries. For practical and economic reasons, the soil container used was of limited size. For the dynamic problem in hand, harmonic waves are generated by the movement of the pile or the suction caissons. The propagating waves will constantly lose energy (mainly radiation damping) until they reach the rigid wall of the container. Upon reflection there (which is theoretically possible), any wave will have such negligible energy that would be unable to change the soil matrix around the foundation. A theoretical assessment is carried out (see Appendix-1) to find the optimum container size based on horizontal wave propagation as proposed by Nogami and Novak (1977). The results showed that, for the suction caisson problems treated herein, the wall boundary effects get diminished after about 5 times the caisson radius. The model tests were carried out in the central part of the chamber to ensure minimal influence due to the wall boundary conditions.

The testing apparatus and the methodology for monopile (Figure 4a) and tetrapod foundation (Figure 4b) can be found in Bhattacharya et al (2012). For the tetrapod structure, the model caissons were 7.4cm in diameter, 5.5cm deep and spaced at 40cm apart in two directions. The other structure (asymmetric tripod, Figure 4c) consisted of three caissons measuring 10cm in diameter by 5cm depth, spaced at an orthogonal distance of 51.5cm centre to centre creating an asymmetric arrangement. The tripod was created following guidance offered by the manufacturer at 1:100 scale. For both the multipod models it was assumed that they would be supporting a standard NREL 5MW wind turbine. This led to two distinctive, and representative wind turbine arrangements.

The overall experimental campaign carried out consists of different types of foundations in various types of soils (dry and saturated fine or coarse sand, saturated clay). However, the model tests reported in this paper were carried out in dry Leighton Buzzard fraction E sand having the following characteristics: silica sand, critical angle of friction  $32^\circ$ ,  $D_{50} = 0.14\text{mm}$ ,  $D_{10} = 0.095\text{mm}$ , maximum and minimum void ratio of 1.014 and 0.613 respectively. As with previous tests, an assessment of the shear modulus of the sand was made using the method proposed by Hardin and Drnevich (1972). For all the sand tests the sand shear modulus remained within the region of 4.0-4.7MPa (measured from mid depth of the caisson). This related to void ratio of about 0.9, which is equivalent to a relative density of 28%.



*Figure 4: Small scale wind turbine model supported on different types of foundation; (a) monopile; (b) symmetric tetrapod foundation; (c) Asymmetric tripod.*

The operational load in a typical wind turbine generates “drained” response in the soil. However, during extreme storm or earthquake, the soil behaviour around the foundation is “partially drained” or in some cases can be “undrained”. As a result, use of dry sand can be justified for operational non-extreme conditions.

Each test was conducted following a standard procedure:

- i. An undisturbed homogeneous sand bed was created for each experiment by dry

- pluviating a body of sand into a stiff box. The density of the sand could be varied by changing the fall height and the aperture diameter in the pluviator.
- ii. The shear modulus of the sand was then calculated allowing an assessment of the foundation stiffness to be made.
  - iii. The turbine model was then carefully installed into the sand matrix under the application of a dead load. Care was taken not to disturb the sand surrounding the caissons.
  - iv. The model was then instrumented with an array of accelerometers and attached to an actuator. The natural frequency was assessed via either a snap back test or a burst of white noise applied to the structure through the actuator. The corresponding acceleration response of the system was used to assess the natural or first modal frequency (FMF) of the structure.
  - v. Using the same actuator a period of cyclic load was applied to the model so as to maintain  $\left(\frac{H}{GD^2}\right)$  non-dimensional group in the range  $10^{-4}$ . Typical load applied is 6N for a tripod in sand. The frequency of the applied loading is so chosen to have  $\left(\frac{f_f}{f_n}\right)$  in the range of 0.85 to 0.9. Typical applied frequency of the loading for the monopile is 3Hz.
  - vi. This loading regime was applied to the structure for a set time period: for most cases this was about an hour. After the forcing regime had been applied the natural frequency was again assessed via either a snap back test or a burst of white noise. The forcing regime was re-applied and the process repeated.
  - vii. After a significant number of cycles had been applied to the structure the forcing regime was stopped and assessment of the natural frequency repeated. The change in FMF with number of cycles could then be analysed.

Figure 5 shows the asymmetric model arrangement in a typical setup. This procedure was repeated a number of times for a number of different lateral loads and forcing frequencies. This procedure was identical for the tripod and it was tested in kaolin clay (having shear modulus of 6MPa). Details of testing of small scale models in clay and the properties of the clay can be found in Bhattacharya et al (2011).

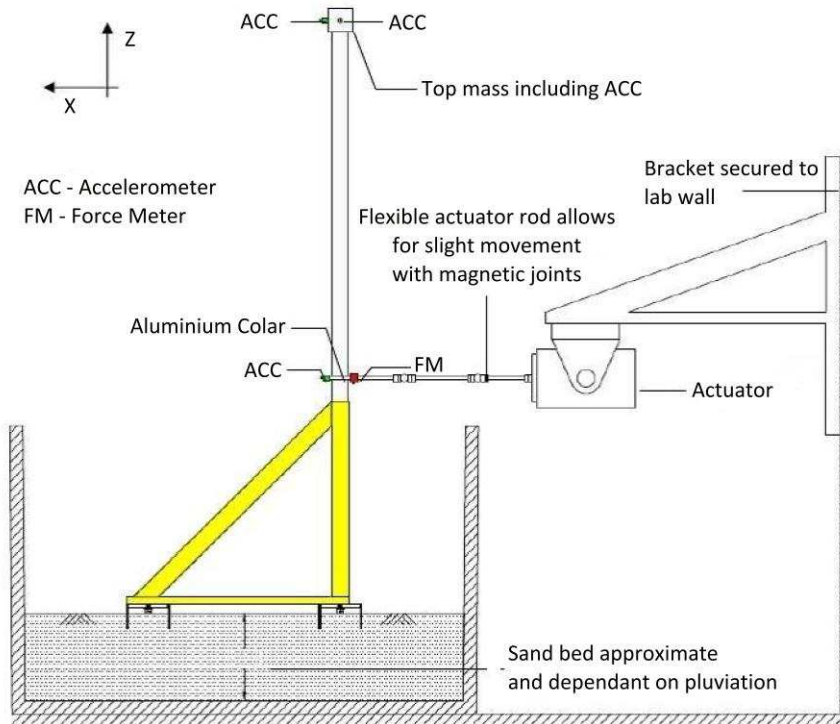


Figure 5: Schematic diagram of the test setup for asymmetric tripod

#### 4.0 RESULTS OF THE TESTS

This section of the paper shows typical free vibration test results from the various setup.

##### ***Free vibration response of a monopile supported wind turbine:***

Figure 6 shows the free vibration data from a typical snap back test performed on a wind turbine with monopile foundation in sand (Figure 4(a)). The test results are plotted in the frequency domain using the Welch (1967) method. The system has a single dominant frequency of about 3.3Hz: the foundation provides significant flexibility to the wind turbine system which has a fixed base frequency of 10.27Hz. A second peak can be observed at about 17Hz which is 5.15 times the first peak and corresponds to the second cantilever mode of the tower. It may be worth noting that the first three modes of vibration of a fixed based cantilever beam are given by:

$$f_n = \frac{1}{2\pi} \alpha_n^2 \sqrt{\frac{EI}{ML^4}} \quad (10)$$

where  $\alpha_n$  is a mode number parameter having the value of 1.875, 4.694, 7.855 for the 1<sup>st</sup>, 2<sup>nd</sup> and 3<sup>rd</sup> mode respectively.  $EI$  is the bending stiffness of the beam having length  $L$  and  $M$  is the mass per unit length of the beam. From equation 10 the ratio of natural frequencies of the first and second modes is 6.26. Our observed ratio of 5.15 results from the flexibility of the foundation.

More details on the dynamics of monopile supported wind turbines are given in Lombardi (2010), Adhikari and Bhattacharya (2011, 2012), Bhattacharya and Adhikari (2011) and Bhattacharya et al (2012). Bhattacharya et al (2012) reported that model

wind turbines founded in sands (both dry and saturated) exhibited stiffening up resulting in an increase in frequency presumably as a result of densification of the soil next to the pile. On the other hand in clay soil, the foundation degraded causing reduction in the frequency of the system with the number of cycles. For foundations in soft clay, the frequency drops as a function of the strain level (the group  $H/GD^2$  in Table 3) in the soil and also the number of loading cycles.

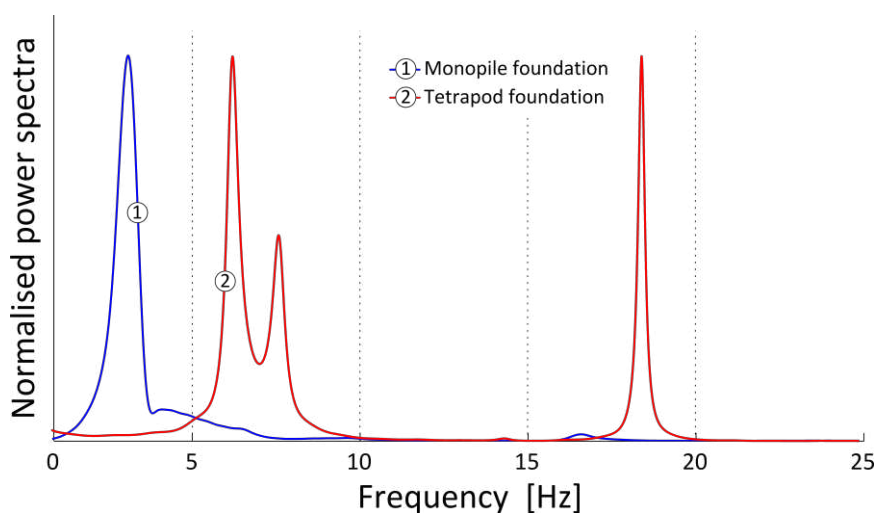


Figure 6: Free vibration response of pile-supported wind turbine and tetrapod-supported wind turbine.

#### **Free vibration response of a symmetric tetrapod supported wind turbine**

Figure 6 also shows a free vibration of a tetrapod supported wind turbine on sand (see Figure 4(b)). Three peaks can be seen in the test results when plotted as spectrum in the frequency domain. These data were recorded just after installation. In contrast to the monopile, there are two very closely spaced peaks at 6.385Hz and 7.754Hz and the third peak is observed at 18.5Hz. The third peak in the tetrapod response is similar to the second peak of the response of a monopile corresponding to the second cantilever mode of the tower. Figure 7 shows the free vibration data of the tetrapod system after 40,500 and 400,000 cycles. The first two peaks gradually converged to form a single peak after about 40,500 cycles until 400,000 cycles when the test was stopped. The final value of this converged frequency was 8.1Hz. It may be concluded that symmetric tetrapod foundations initially responded in two different natural frequencies and the two spaced values after intensive repetitive loading converged into a single one, that seemed unchanged over time. It was verified by accelerometers in two orthogonal directions that this effect owes to the fact that the lowest modes in the two principal vibration axes are detuned (i.e. having different frequencies) and get progressively tuned while cyclically being excited with the operational load. A plausible reason is that the loads get continuously redistributed in the four supports until homogeneity of how the load spreads around is reached i.e. all caissons attain the same stiffness.

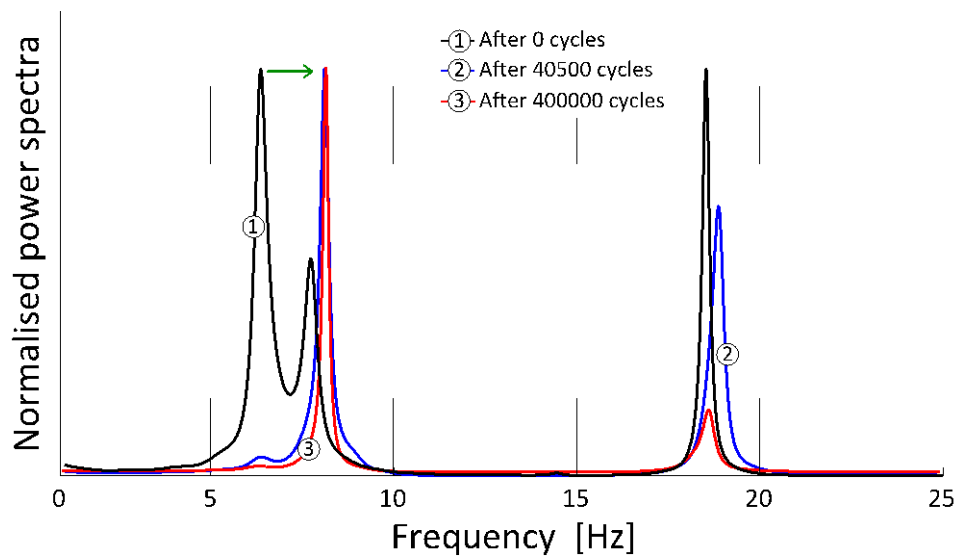


Figure 7: Cumulative results for snap-back test on the tetrapod supported wind turbine model on sand

#### **Free vibration response of an asymmetric tripod supported wind turbine:**

Figure 8 shows a typical free vibration response of three scaled asymmetric tripods in sand where it can be clearly seen that there are two closely spaced peaks at all the three scales. This observation of two closely spaced peaks is quite similar to the symmetric tetrapod as presented in Figure 6. Figure 9 shows a typical free vibration response of a 1:150 scale model in clay where two peaks can also be observed. In order to understand the reason behind the two peaks, the free vibration test was carried out on the same 1:150 scaled model whereby two accelerometers were oriented in their principle axis (see by X-X' and Y-Y' on the inset of Figure 10). This test confirmed that these modes are due to the rocking motion of the entire system in two principle axis (X'-X' and Y'-Y' in Figure 11) and the values of the frequency are different. This phenomenon was further confirmed through a numerical study as shown in Figure 11. Figure 11 shows the output from a numerical analysis showing the first two modes of vibration.

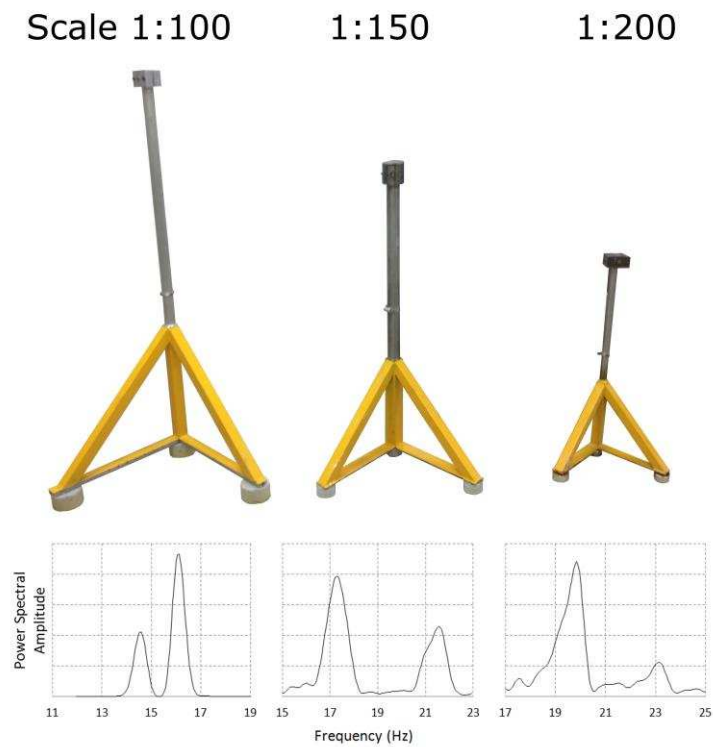


Figure 8: Typical test result from snap-back test on the asymmetric tripod on sand.

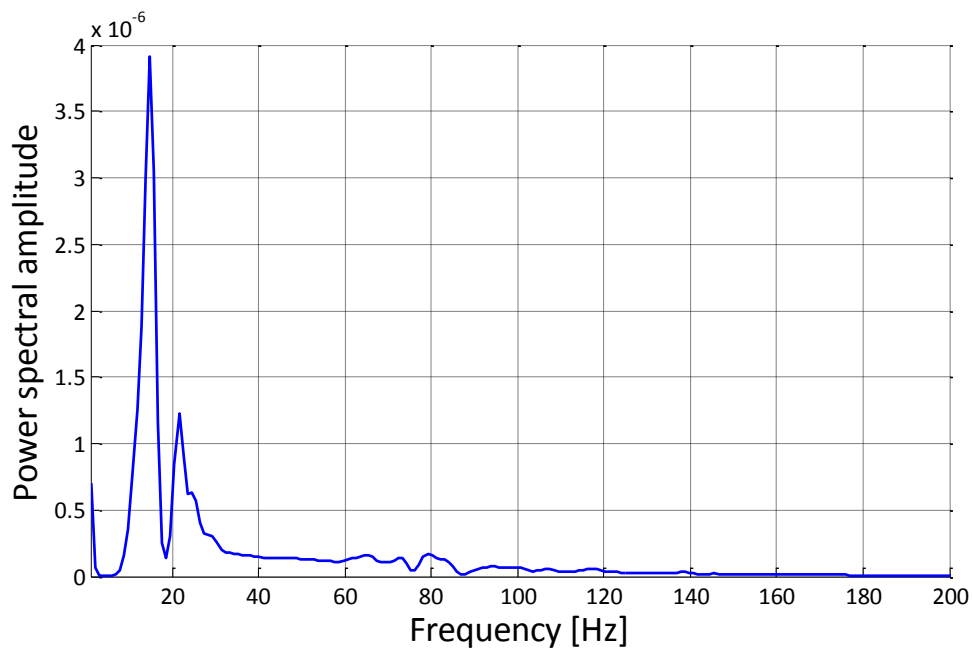


Figure 9: Typical test of asymmetric tripod on kaolin clay

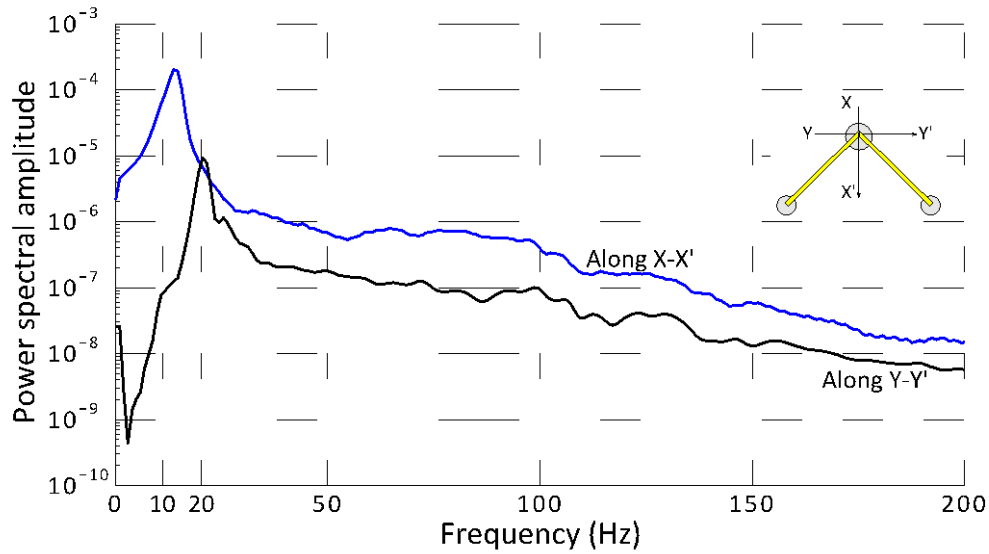


Figure 10: Typical test result from snap-back test on tripod supported wind turbine model on clay

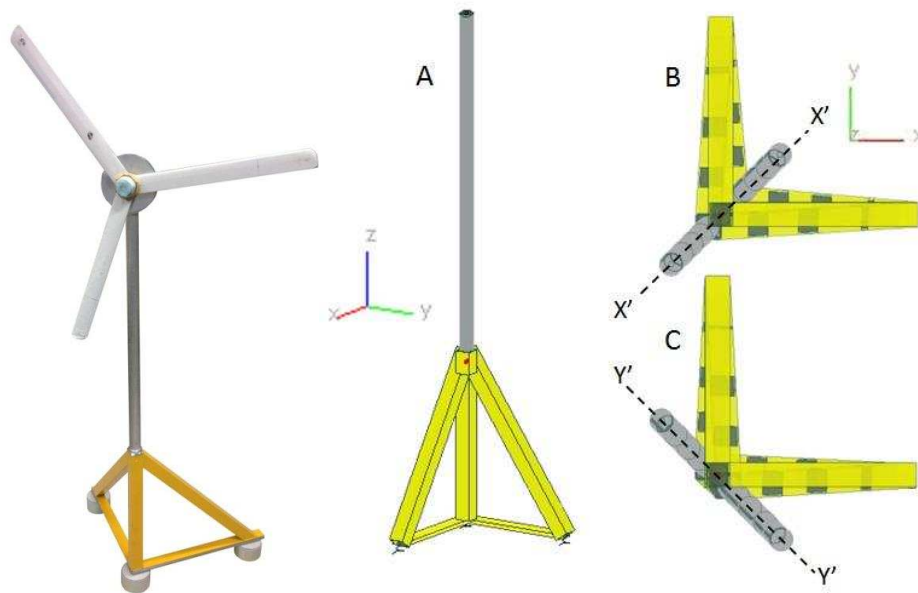


Figure 11: Modes of Vibration of the asymmetric tripod

The scaled models were then subjected to millions of cycles and the change in dynamic characteristics were monitored through white noise testing and/or snap back testing. Figure 12 shows the progressive change in dynamic characteristics of the system after 400,000 cycles, 800,000 cycles, 1.2M and 1.6M cycles. It is interesting to note that the tripod arrangement persistently maintained two closely spaced frequencies throughout testing. Furthermore, the lower peak shifts towards the right indicating a strain-stiffening behaviour. This behaviour is in contrast to the symmetric tetrapod behaviour where the two peaks converged to form a single peak, the reasons for which is explored in the next section.

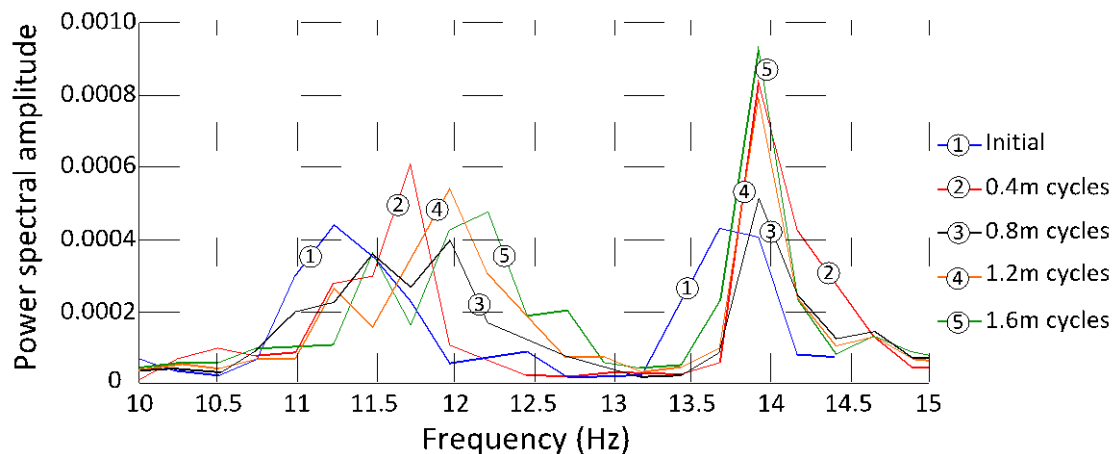


Figure 12: Typical test result from snap-back test on asymmetric tripod supported wind turbine model on sands in steps of 400,000 cycles of loading.

## 5.0 MULTIPOD DYNAMIC BEHAVIOUR AND MODELLING

Evaluation of the first natural frequency of the wind turbine system is critical for avoiding resonant response and subsequent excessive vibration amplitudes that may deteriorate fatigue performance. Multipod arrangements have been customarily treated dynamically in the same way as monopiles (Zaaijer 2003), while comparative approaches assessing the relative merits of different types of foundations have centred on response far from the operational dynamic characteristics (Schaumann *et al.* 2011). The observed behaviour in the scale tests reported in this paper is quite distinct, indicating a salient feature never previously reported for offshore multipod foundations. They are: (a) Multipod foundations have two peak responses i.e. two closely spaced natural frequencies due to the combination of rigid rocking modes and the flexible modes of the tower; (b) The natural frequencies of wind turbine supported on multipod foundations change with repeated cycles of loading; (c) There is a convergence of peaks for symmetric tetrapod but not for asymmetric tripod.

An explanation for such an observation can be obtained from standard lumped mass discrete models, where the foundation caissons are replaced by linear springs and dashpots as in Andersen *et al.* 2009. For the present case, frequency-independent springs have been assumed and the damping parameters, not being essential for the current analysis, were set without any loss of generality to zero. Figure 13 illustrates such discrete modelling realisations for the tetrapod and tripod foundations, when decoupling the planar motions along the principal axes X and Y. Assuming homogeneity across the soil substrate each caisson is assigned an identical spring of vertical stiffness  $K_v$  both in tension (uplift) and compression. All springs are connected to the top mass through a rigid beam. Writing the undamped equations of motion in the XZ and YZ plane for both cases it can be seen that the effect of the rigid beam rocking (i.e. rotation  $\theta$ ) is different for the two planes when considering the tripod solution. Different dynamic and static coupling exists, consequently leading to different modal frequencies out of the relevant eigenvalue problem.

In contrast, the symmetry of the square tetrapod will produce identical frequencies in the two orthogonal vibration planes considered. Any deviation from a single frequency motion initially observed during tetrapod testing should be the result of slight disparities in the symmetry of the arrangement, for example the spatial variability of soil causing different values of  $K_V$  for the four caissons. These disparities could affect the initial values of spring stiffness ( $K_V$ ) but under repeated cyclic loading they converge to a constant value. The loads become redistributed and the amplitude of vibrations stiffens the sand matrix eventually making the values of  $K_V$  converge and the two closely spaced natural frequencies converge to form a single peak as shown in Figure 7.

Any asymmetric multipod foundation (e.g. tripod or rectangular) will also produce two low natural frequencies. However in this case, they are not expected to merge to form a single peak due to the fact that the natural frequency in the two principal planes (XZ and YZ) are not same. Due to strain stiffening effects i.e. compaction/densification of the soil around the caissons, the lower peak moved to the left but they did not merge (see Figure 12). This is in contrast to the symmetric tetrapod where the two peaks merged to form a single peak. This particular aspect warrants further investigation and consideration when designing such foundation structures.

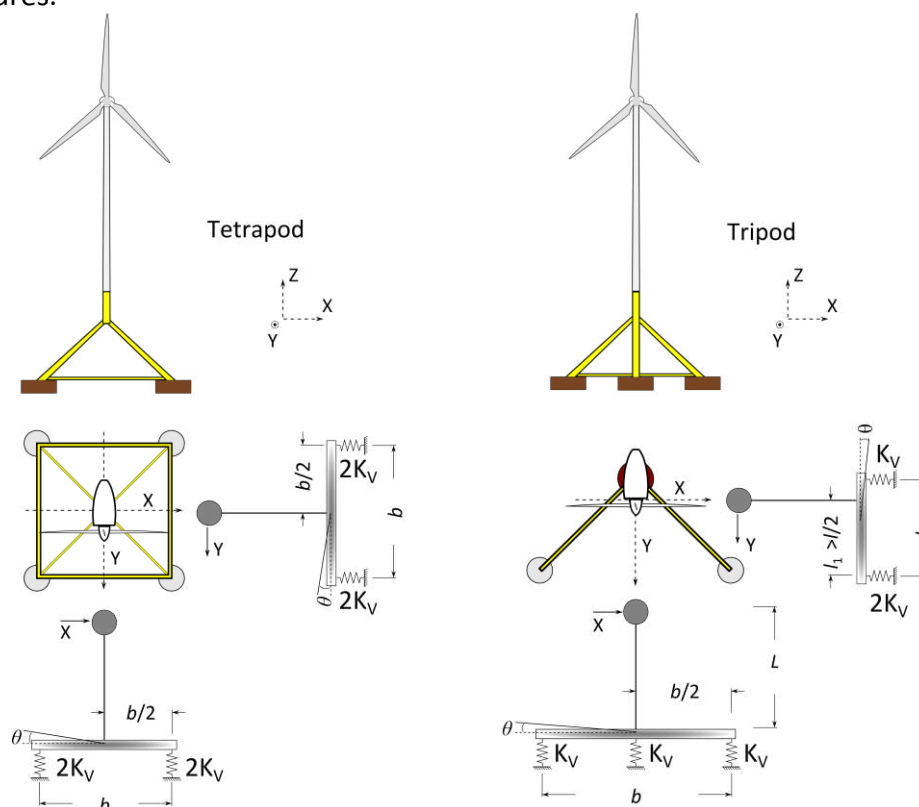


Figure 13: Lumped mass modelling of the tetrapod and tripod foundation solutions. For the two different cases, the influence of elastic foundations is inherently different along the two principal vibration axes.

Earlier it was quoted that the DNV guidelines require that the wind turbine fundamental frequency lies in a narrow band between the 1P and 3P frequency values. Yet in the case of two frequencies with a ratio between them ranging between 1.2 and 1.5, as was the case here for a tripod arrangement the task of fitting both of them in a safe zone far from resonance becomes more difficult. This aspect is shown in Figure 14 where the various forcing powers are plotted along with the frequencies. This upper panel of the figure shows schematically the four types of loading, wind, wave, blade rotational excitation (1P) and the interruption of wind caused by blade passing (3P). Vortex shedding and other complex aerodynamic phenomena are not displayed in the figure. The wind spectrum is the lowest frequency followed by the waves spectrum that has a marginally higher frequency content. The blade rotational excitation is shown as a typical monochromatic frequency with sidelobes caused by windowing. The blade passing is idealised as a periodic boxcar function whose Fourier spectrum is a spike at 3P and all integer multiples of 3P.

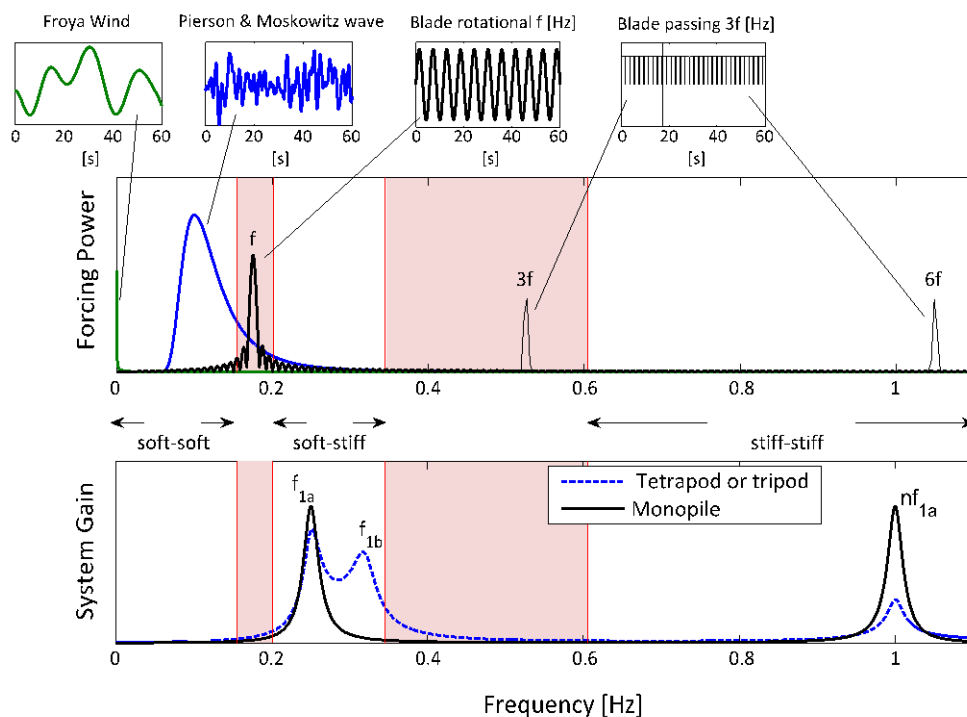


Figure 14: Relationship between effect of natural frequency of suction caisson and monopile on the forcing frequencies

On the other hand, the lower panel of the figure shows the frequency response function of a hypothetical design in the soft-stiff band. The monopiled structure has a single peak in the FRF (Frequency Response Function) at  $f_{1a}$ . This is in contrast to the tripod structure that has two closely spaced peaks  $f_{1a}$  and  $f_{1b}$ . These two peaks inevitably broaden the range of frequencies that can be excited by the loading. The possibility of coincidence of  $6f$  (the first harmonic of blade passing) and the second/third peak of the system FRF is also a potential concern. This also may coincide with the blade natural frequency which is about 1Hz. In this context, it may be noted that according to current suggestions for tripod arrangement

characteristics (de Vries 2011) the second natural frequency encountered would always fall in the 3P zone.

## **CONCLUSIONS:**

Offshore wind turbines are dynamically sensitive structures as a result of the mass distribution along their length and also because the forcing frequencies of the applied loads are close to their natural frequencies. A so-called “soft-stiff” system is used in practice whereby the global fundamental frequency of the overall wind turbine-foundation system is chosen to lie in the interval between turbine and blade passing frequencies which may be a very narrow band, typically between 0.22Hz and 0.31Hz. It has been demonstrated that the natural frequency of the overall system shifts (i.e. decreases or increases) with cycles of loading due to stiffening or softening of the foundation system. Between 7% and 24% change in natural frequency can be allowed for a wind turbine system depending on the make of the turbine (figures correspond to the five representative cases selected herein) and in the absence of very reliable site characteristics, that is knowledge of whether the foundation system will stiffen or soften.

Results from scaled models of multipod (tetrapod and asymmetric tripod) supported wind turbines showed quite distinct behaviours, indicating a salient feature never previously reported for such offshore foundations. The response of monopile systems in sand will be governed by the the large number of repeated cycles of lateral load, which lead to compaction and stiffening of the system. On the other hand, multipod foundations’ behaviour will be governed by rocking motions and the redistribution of forces in the supporting pods. Specific conclusions derived from the study are summarised below:

1. Wind turbines on multipod foundation will have two closely spaced natural frequencies corresponding to rocking modes of vibration. These two close frequency values are effectively the first natural frequency in two principle vibration axes. This is in contrast to the monopile foundation system where a single spectral peak will be observed in the response power spectrum and the second peak, (resulting from the second bending mode of the tower) will typically be located at a natural frequency about 5 times higher.
2. The closely spaced spectral peaks for multipod foundations shift with cycles of loading as a result of the soil-structure interaction. Therefore dynamic soil-structure interaction is an important design consideration to predict the short and long term performance of these structures.
3. The responses of a symmetric tetrapod and an asymmetric tripod under long term cyclic loading are very different. For a symmetric tetrapod, the first two closely spaced spectral peaks converge to form a single peak after tens of thousands of cycles. On the other hand, for the asymmetric tripod, the two closely peaks do not converge even after being subjected to 1.6M cycles.

**Acknowledgements:** The authors would like to thank the following project students: Anabel Young, Bretton Davies, Hannah Steedman, Maria Benjaminsdottir, Sina Zeraati and Samuel Scott for their enthusiasm in carrying out many of the tests. The authors also acknowledge the excellent technical support obtained from Clive Rendall and Tony Griffiths. Necessary funding for carrying out these tests was obtained from RWE Innogy.

### Appendix-1: Assessment of chamber size effects for dynamic soil-structure interaction testing of wind turbines

For technical reasons, the soil container used throughout the experimental campaign is of limited size. An assessment is therefore necessary to find the optimum dimension that may be required. This appendix reports a theoretical study to find such a size specification.

A cylindrical section of radius  $r_p$  (suction caisson radius) is embedded in a soil and the soil layer is excited by horizontal harmonic motion (having unit amplitude and frequency  $\omega$ ) of the suction caisson. A cylindrical coordinate system  $(r, \theta, z)$  representation has been used to study the problem. Using potential functions related to longitudinal and shear waves, Nogami and Novak (1977) derived the expressions for displacements and stresses in the soil for a similarly shaped pile. The amplitudes  $u$  (in radial  $r$  direction) and  $v$  (in  $\theta$  direction) for soil displacement due to the imposed harmonic motion are represented as a series of infinite terms, each given by equations A(i) and A(ii), corresponding to the infinite modes that are excited in the soil.

$$u_n(r, \theta, z) = -\cos \theta \cdot \sin h_n z \cdot \left\{ A_n \left[ \frac{1}{r} K_1(q_n r) + q_n K_0(q_n r) \right] - B_n \left[ \frac{1}{r} K_1(s_n r) \right] \right\} \quad (\text{Ai})$$

$$v_n(r, \theta, z) = -\cos \theta \cdot \sin h_n z \cdot \left\{ A_n \left[ \frac{1}{r} K_1(q_n r) \right] - B_n \left[ \frac{1}{r} K_1(s_n r) + s_n K_0(s_n r) \right] \right\} \quad (\text{Aii})$$

where  $h_n$ ,  $q_n$  and  $s_n$  are given by equations (18) in Nogami and Novak (1977) and  $K_1(q_n r)$ ,  $K_1(s_n r)$ ,  $K_0(q_n r)$  and  $K_0(s_n r)$  are modified Bessel functions of order  $n$ . It can be easily shown that the functions  $K_1(q_n r)$ ,  $K_1(s_n r)$ ,  $K_0(q_n r)$  and  $K_0(s_n r)$  converge to zero for  $|q_n r| \rightarrow \infty$  and  $|s_n r| \rightarrow \infty$  (Abramowitz and Stegun 1965) and present their minimum values at  $n = 1$ .  $A_n$  and  $B_n$  are given by equations (22) in Nogami and Novak (1977). On this basis, one can evaluate the convergence rates for the soil displacement modal amplitudes  $u_n$  and  $v_n$  for various values of the radius  $r$  (when assuming unit modal amplitude values  $u_{n0}$  and  $v_{n0}$ ).

#### **Results for the suction caisson supported tetrapod and tripod tests**

Figures A1(a) and (b) show the results of analysis for a tetrapod suction caisson case, which has diameter 7.4cm and depth 5.5cm; the first 4 modes are shown.

The results indicate that any wall boundary effects get negligible at about 5 times the suction caisson radius.

Figures A2(a) and (b) show the results of analysis for a tripod's suction caisson having 10cm diameter and 5cm depth; again the first 4 modes are shown. The results very similar to before illustrate the absence of wall boundary effects at less than 5 times the radius of the suction caisson.

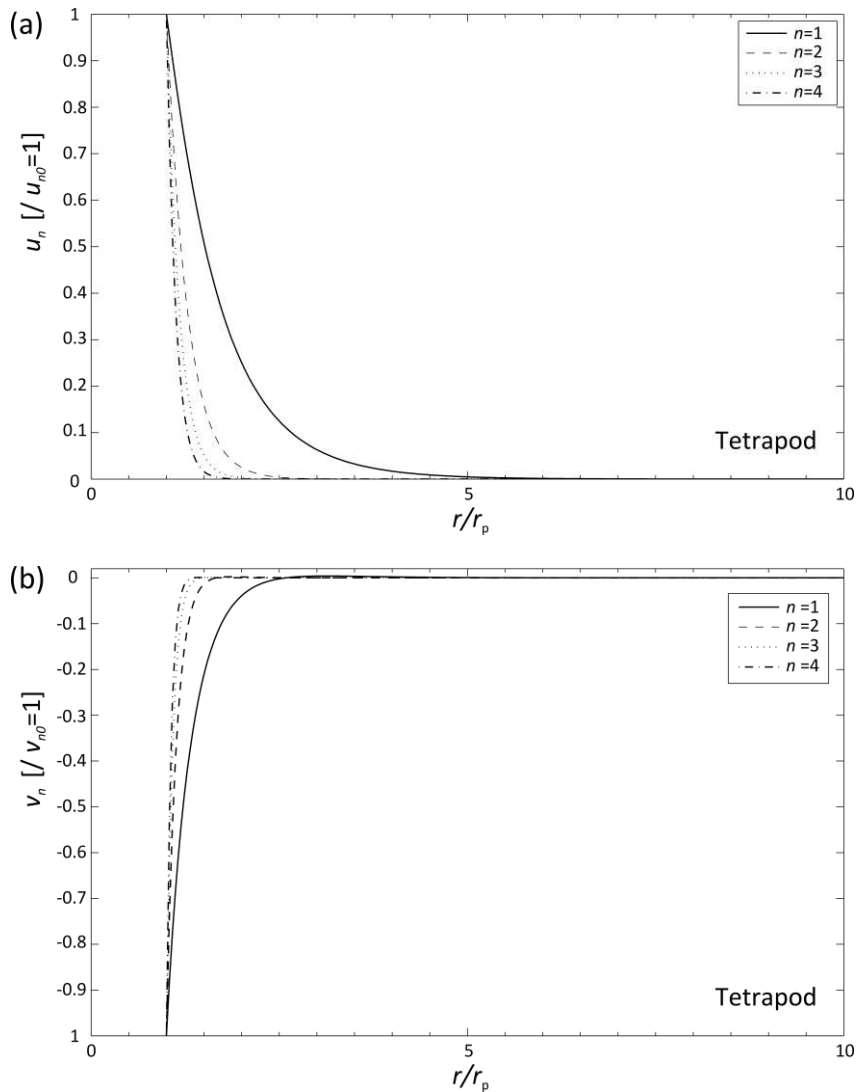


Figure A1: (a) Radial displacement of the soil for the tetrapod case, (b) Circumferential displacement of the soil for the tetrapod case

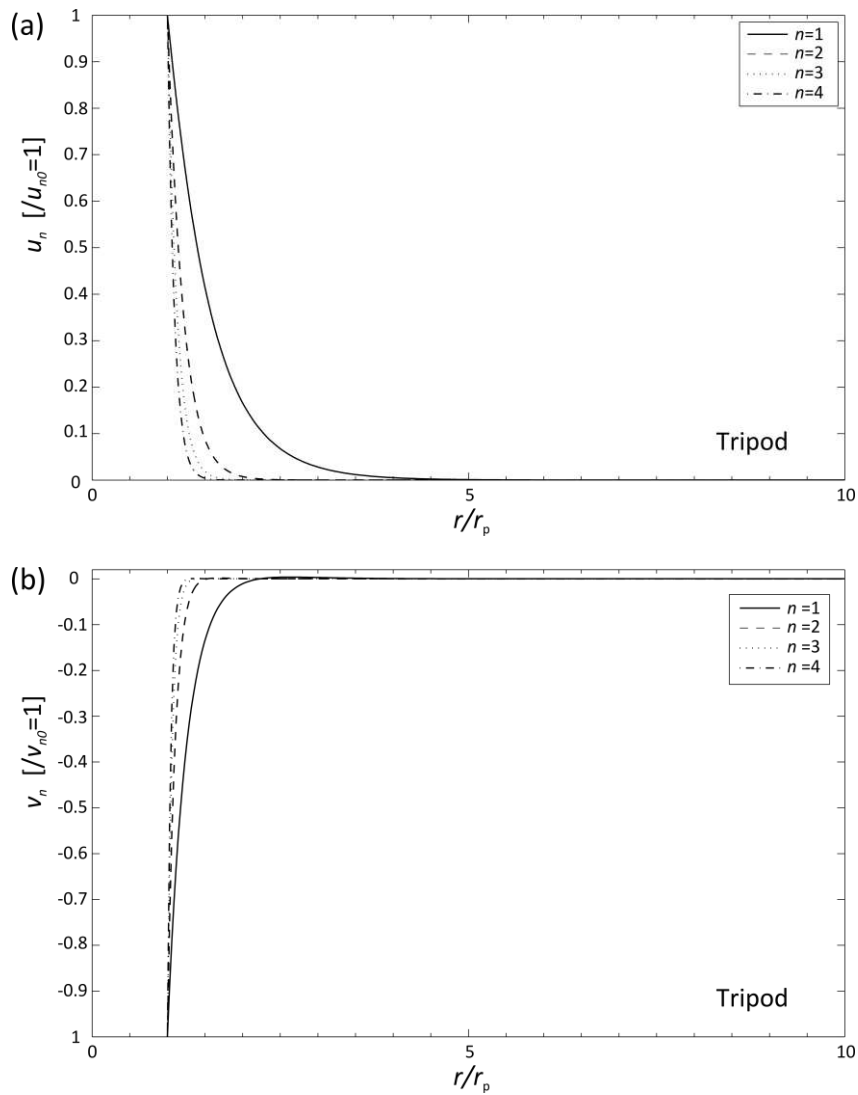


Figure A2: (a) Radial displacement of the soil for the tripod case , (b) Circumferential displacement of the soil for the tripod case

**References:**

1. Achmus M, Kuo YS, Abdel-Rahman K. Behavior of monopile foundations under cyclic lateral load. *Computers and Geotechnics* 2009; 36(5):725–735.
2. Adhikari S, Bhattacharya S. Dynamic analysis of wind turbine towers on flexible foundations. *Shock and Vibration* 2012; 19:37-56.
3. Adhikari S, Bhattacharya S. Vibrations of wind-turbines considering soil-structure interaction. *Wind and Structures - An International Journal* 2011; 14:85-112.
4. Andersen L, Ibsen LB, Linaard MA. Lumped-parameter model of a bucket foundation. In Nielsen SA, editor, *Joint Research and Development: Innovative Foundation Solutions*, MBD Offshore Power A/S and Aalborg University, Aalborg, 2009.
5. Abramowitz M, Stegun I. *Handbook of Mathematical functions*, Dover, 1965.

6. Bhattacharya S, Lombardi D, Muir Wood DM. Similitude relationships for physical modelling of monopile- supported offshore wind turbines. *International Journal of Physical Modelling in Geotechnics* 2011; 11(2):58-68.
7. Bhattacharya S, Adhikari S. Experimental validation of soil–structure interaction of offshore wind turbines. *Soil Dynamics and Earthquake Engineering* 2011; 31(5-6):805-816.
8. Bhattacharya S, Cox J, Lombardi D, Muir Wood D. Dynamics of offshore wind turbines supported on two foundations. *Geotechnical engineering: Proceedings of the ICE* 2012; 166(2):159-169.
9. Cox J, Jones C, Bhattacharya S. Long term performance of suction caisson supported offshore wind turbines. *The Structural Engineer* 2011; 89(19):12-13.
10. Cuéllar P, Georgi S, Baeßler M, Rücker W. On the quasi-static granular convective flow and sand densification around pile foundations under cyclic lateral loading. *Granular Matter* 2012; 14(1):11-25.
11. De Vries W. Support structure concepts for deep water sites. EU Project UpWind, final report WP 4.2, Delft University of Technology, the Netherlands; 2011.
12. DNV (Det Norske Veritas) 2002 Guidelines for Design of Wind Turbines, 2<sup>nd</sup> edition DNV, London, UK.
13. Doherty JP, Houlsby GT, Deeks AJ. Stiffness of flexible caisson foundations embedded in non-homogeneous elastic soil. *Journal of Geotechnical and Geoenvironmental Engineering* 2005; 131(12): 1498-1508.
14. EWEA. The European offshore wind industry key 2011 trends and statistics. Brussels: 23; 2012.
15. Hardin BO, Drnevich VP. Shear modulus and damping in soils: design equations and curves. *Journal of the Soil Mechanics and Foundations Divisions, ASCE* 1972; 98(7):667-692
16. Kühn M. Dynamics of offshore wind energy converters on monopile foundations- experience from the Lely offshore wind farm. EPSRC workshop report on OWEN (Offshore Wind Energy Network) [http://www.owen.org.uk/workshop\\_3/martin\\_kuehn\\_1.pdf](http://www.owen.org.uk/workshop_3/martin_kuehn_1.pdf) ; 2000.
17. Kuo Y, Achmus M, Abdel-Rahman K. Minimum embedded length of cyclic horizontally loaded monopiles. *Journal of Geotechnical and Geoenvironmental Engineering* 2012; 138(3):357–363.
18. Lombardi D, Bhattacharya S, Muir Wood D. Dynamic soil-structure interaction of monopile supported wind turbines in cohesive soil. *Soil Dynamics and Earthquake Engineering* 2013; 49:165-180.
19. Lombardi D. Dynamics of offshore wind turbines. MSc Thesis, University of Bristol, 2010.
20. Nogami T, Novak M. Resistance of soil to a horizontally vibrating pile. *International Journal of Earthquake Engineering and Structural Dynamics* 1977; 5:249-261.
21. Schaumann P, Lochte-Holtgreven S, Steppeler S. Special fatigue aspects in support structures of offshore wind turbines, *Materialwissenschaft und Werkstofftechnik* 2011; 42(12):1075-1081.

22. Welch PD. The use of fast Fourier transform for the estimation of power spectra: A method based on time averaging over short, modified periodograms. IEEE Transactions on Audio and Electroacoustics 1967; 15(2):70-73.
23. Zaijier MB. Foundation models for the dynamic response of offshore wind turbines. In: International Conference on Marine Renewable Energy (MAREC), Newcastle, UK; 2002.
24. Zaijier MB. Comparison of monopile, tripod, suction bucket and gravity base design for a 6 MW turbine. In: Proceedings of the OWEMES 2003 Conference, Naples, Italy; 2003.